Liquid Crystals
Publication details, including instructions for authors and subscription information:
http://www.informaworld.com/smpp/title~content=t713926090

Cholesteric star-shaped liquid crystals induced by a maltose core: synthesis and characteristics

Mei Tian[a]; Bao-Yan Zhang[a]; Yue-Hua Cong[a]; Xiao-Zhi He[a]; Hui-Shu Chu[a]; Xiao-Yu Zhang[a]
[a] Centre for Molecular Science and Engineering, Northeastern University, Shen-yang, People's Republic of China

To cite this Article Tian, Mei , Zhang, Bao-Yan , Cong, Yue-Hua , He, Xiao-Zhi , Chu, Hui-Shu and Zhang, Xiao-Yu(2010) 'Cholesteric star-shaped liquid crystals induced by a maltose core: synthesis and characteristics', Liquid Crystals, 37: 11, 1373 — 1379

To link to this Article: DOI: 10.1080/02678292.2010.517325

URL: http://dx.doi.org/10.1080/02678292.2010.517325

Liquid Crystals,
Vol. 37, No. 11, November 2010, 1373–1379

Cholesteric star-shaped liquid crystals induced by a maltose core: synthesis and characteristics

Mei Tian, Bao-Yan Zhang*, Yue-Hua Cong, Xiao-Zhi He, Hui-Shu Chu and Xiao-Yu Zhang

Centre for Molecular Science and Engineering, Northeastern University, Shen-yang 110004, People's Republic of China

(*Received 21 January 2010; final version received 13 April 2010*)

Three esters of maltose (**A1**–**A3**) with 4–(4–(alkoxybenzoyloxy)phenoxy) –6–oxohexanoic acid (**b1**–**b3**) side-arms have been synthesised. All the maltose derivatives were laevo-rotationary, unlike their parent cores. The side arm **b1** did not display liquid crystalline (LC) properties, and **b2** and **b3** displayed thermotropic nematic LC properties. The star-shaped compound (SSC) **A1** with **b1** side-arms did not display a mesomorphic phase. Unlike the nematic schlieren texture provided by side-arms **b2** and **b3**, the star-shaped liquid crystals (SSLC) **A2** and **A3** displayed Grandjean and oily texture in the cholesteric phase. The results suggest that the LC properties of the side-arms have an important influence on the formation of LC properties in an SSC, and that the maltose core is important in determining the mesomorphic phase type. In other words, the SSC displayed LC properties only when the side-arms were also LC, and the maltose core induced a cholesteric phase in the SSLC with nematic side-arms. The mesomorphic regions for **A2** and **A3** were 39.1 and 53.7°C during the heating cycle and 63.8 and 107.0°C during the cooling cycle, respectively. The longer terminal chain rendered the mesomorphic region broader.

Keywords: star-shaped liquid crystal; maltose; cholesteric phase; nematic arms

1. Introduction

Cholesteric liquid crystals (LCs) possessing the unique properties of selective reflection, high optical rotation power and circular dichroism offer considerable potential for a variety of optical applications [1–4]. One type of unconventional LC, those possessing a star-shaped molecular structure, usually comprise a core and a small number of mesomorphic units as side-arms. These have attracted interest on account of their symmetrical molecular structure and their interesting optical properties [5–32]. The common mesophase of star-shaped liquid crystals (SSLC) is columnar. To the best of our knowledge, cholesteric SSLCs have been described only rarely in the past. However, Yao *et al.* [5], Saezz and Goodby [10] and Zhang *et al.* [31] have introduced cholesteric mesomorphic arms into a flexible core and obtained cholesteric SSLCs. In these cases, the cholesteric mesomorphic phase of the SSLC was mainly the result of cholesteric mesomorphic arms.

The question we have asked ourselves is whether cholesteric mesomorphic arms are essential for the formation of cholesteric SSLCs. Might a cholesteric SSLC be generated by a chiral core? Over the past two years we have focused on this topic. Glucose, sorbitol and melitose had previously been used as chiral cores in the synthesis of cholesteric SSLCs [33, 34]. Our results now indicate for the first time that glucose, melitose and sorbitol are able to induce a cholesteric phase in SSLCs containing nematic LC side-arms. It was instructive to synthesise various types of cholesteric SSLC based on different chiral cores in order to assess their properties and explore their potential applications. In the present paper, three maltose derivates (**A1**–**A3**) are described, containing side-arms, **b1**, **b2** or **b3,** respectively. The molecular structure is illustrated in Scheme 1. The properties of **A1**–**A3**, and the influence of the chiral core on the properties of the SSLC have been studied and are discussed.

2. Experimental

2.1 *Materials and measurements*

Benzoic acid, 4-methoxybenzoic acid, 4-ethoxybenzoic acid, hydroquinol and anhydrous maltose were obtained from Beijing Chemical Industry Company (China). Hexanedioic acid, thionyl chloride, pyridine and tetrahydrofuran were purchased from Shenyang Chemical Industry Company (China). N,N′-dicyclohexylcarbodiimide (DCC) and 4-dimethylaminopyridine (DMAP) were bought from Shanghai Chemical Industry Company (China). All solvents were purified by conventional methods.

2.2 *Characterisation*

FT–IR spectra were determined on a Spectrum One (B) spectrometer (Perkin–Elmer, Foster City, CA, USA). Proton nuclear magnetic resonance (^{1}H NMR) spectra (300 MHz) were obtained with a Gemini 300

---

*Corresponding author. Email: baoyanzhang@hotmail.com

ISSN 0267-8292 print/ISSN 1366-5855 online

DOI: 10.1080/02678292.2010.517325
http://www.informaworld.com

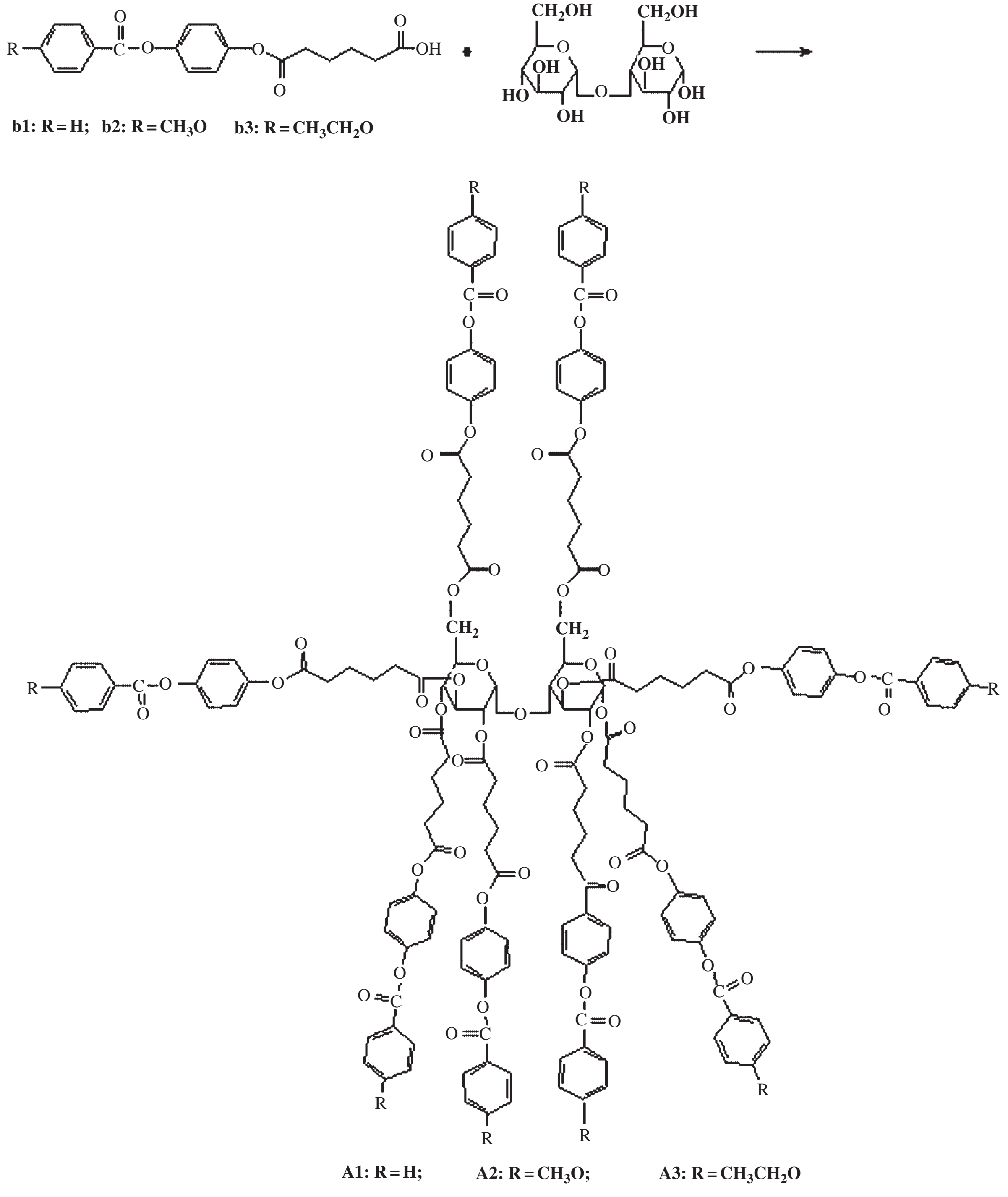

Scheme 1. Synthesis of star-shaped compounds **A1**–**A3**.

spectrometer (Varian Associates, Palo Alto, CA). The elemental analyses were carried out on an Elementar Vario EL III (Elementar, Hanau, Germany). Phase transition temperatures and thermodynamic parameters were determined by means of a DSC 204 (Netzsch, Selb, Germany) equipped with liquid nitrogen cooling system. The heating and cooling rates were 10°C min^{-1} under a nitrogen atmosphere. The thermal transition temperatures were recorded during the first heating and cooling cycle. A DMRX polarising optical microscope (Leica, Wetzlar, Germany) equipped with THMSE–600 hot stage (Linkam, Surrey, England) under a nitrogen atmosphere was employed to observe phase transition temperatures and optical textures.

X-ray diffraction (XRD) measurements were performed with nickel-filtered Cu–Kα (λ = 1.52 Å) radiation using a DMAX–3A powder diffractometer (Rigaku, Tokyo, Japan). The optical activity of the SSLCs was determined on a Perkin–Elmer Model 341 polarimeter; measurements were carried out in tetrahydrofuran (THF) in a 2 mL cuvette, 100 mm in length, using sodium light at λ = 589 nm.

2.3 Synthesis

2.3.1 4-(4-(alkoxybenzoyloxy)phenoxy)-6-oxohexanoic acid (b1–b3)

Compounds **b1**–**b3** were prepared using procedures described previously [33].

2.3.2 Octo[4-(4-(alkoxybenzoyloxy)phenoxy)-6-oxohexanoic acid] maltose ester (A1–A3)

A1, **A2** and **A3** were prepared by a similar synthetic procedure. The synthesis of **A3** is given as an example. A solution of anhydrous maltose (0.36 g, 1 mmol) in dry pyridine (20 ml) was added to a solution of **b3** (3.088 g, 8 mmol) in dry pyridine (60 ml) containing DCC (1.648 g, 8 mmol) and DMAP (0.244 g, 2 mmol). The reaction mixture was stirred for 72 h at room temperature and filtered. The filtrate was poured into water and acidified with dilute hydrochloric acid. The crude product was filtered off and washed with water to neutral pH, and finally washed with ethanol. The product was dissolved in petroleum ether and chromatographed on a silica gel column using petroleum 5/1 ether/ethyl acetate as eluent, yielding a white powder (0.69 g, 21%). Properties of **A1**, **A2** and **A3** were as follows.

A1: Yield, 18%; m.p. 169.4°C.
Elemental analysis. Calculated for $C_{164}H_{150}O_{51}$: C, 67.08; H, 5.11%. Found: C, 66.84; H, 5.34%.
IR (KBr, cm^{-1}): 2928, 2852 ($–CH_2–$), 1752–1716 (C=O), 1610, 1510 (–Ar), 1250, 1043 (C–O–C).
^{1}H NMR ($CDCl_3$, TMS, δ, ppm): 1.555–1.581 (m, 32H, $–CH_2–$), 2.380–2.641 (m, 32H, $–CH_2–$), 4.321–5.660 (m, 12H, H–pyranose ring), 5.750 (d, 1H, J = 6.6 HZ), 6.561 (d, 1H, J = 3.5 Hz), 7.113–7.134 (m, 16H, Ar–H), 7.205–7.228 (m, 16H, Ar–H), 7.366–7.375 (m, 24H, Ar–H), 8.136–8.158 (m, 16H, Ar–H).

A2: Yield, 23%; m.p. 148.7°C.
Elemental analysis. Calculated for $C_{172}H_{166}O_{59}$: C, 65.03; H, 5.23%. Found: C, 64.79; H, 5.62%.
IR (KBr, cm^{-1}): 2975, 2846 ($–CH_3$, $–CH_2–$), 1757–1716 (C=O), 1608, 1506 (–Ar), 1265, 1044 (C–O–C).
^{1}H NMR ($CDCl_3$, TMS, δ, ppm): 1.778–1.806 (m, 32H, $–CH_2–$), 2.423–2.460 (m, 16H, $–CH_2–$), 2.568–2.591 (m, 16H, $–CH_2–$), 3.742–3.803 (m, 24H, $CH_3O–$), 4.331–5.674 (m, 12H, H–pyranose ring), 5.756 (d, 1H, J = 6.6 HZ), 6.560 (d, 1H, J = 3.5Hz), 6.951–6.973 (m, 16H, Ar–H), 7.111–7.137 (m, 16H, Ar–H), 7.201–7.224 (m, 16H, Ar–H), 8.115–8.147 (m, 16H, Ar–H).

A3: Yield, 21%; m.p. 133.1°C.
Elemental analysis. Calculated for $C_{180}H_{182}O_{59}$: C, 65.73; H, 5.54%. Found: C, 65.04; H, 5.67%.
IR (KBr, cm^{-1}): 2971, 2856 ($–CH_3$, $–CH_2–$), 1747–1718 (C=O), 1614, 1500 (–Ar), 1271, 1042 (C–O–C).
^{1}H NMR ($CDCl_3$, TMS, δ, ppm): 1.443–1.475 (m, 24H, $–CH_3$), 1.792–1.812 (m, 32H, $–CH_2–$), 2.424–2.463 (m, 16H, $–CH_2–$), 2.586–2.620 (m, 16H, –CH2–), 4.096–4.154 (m, 16H, $–CH_2O–$), 4.334–5.677 (m, 12H, H–pyranose ring), 5.752 (d, 1H, J = 6.6 HZ), 6.561 (d, 1H, J = 3.5 Hz), 6.954–6.971 (m, 16H, Ar–H), 7,117–7.141 (m, 16H, Ar–H), 7.202–7.225 (m, 16H, Ar–H), 8.111–8.149 (m, 16H, Ar–H).

3. Results and discussion

3.1 Synthesis

The SSCs, **A1**, **A2** and **A3**, were synthesised by esterification with DCC as dehydration agent and DMAP as catalyst. Their structural characteristics were in agreement with those predicted.

In **A1**–**A3**, the disappearance of the characteristic –OH and –COOH bands at 3260–2500 and 1708 cm^{-1} indicated that the side-arms **b1**–**b3** had been successfully incorporated to maltose. The absorption bands of **A1**–**A3** were as follows:
2975–2846 cm^{-1} ($–CH_3$, $–CH_2–$), 1757–1716 cm^{-1} (C=O stretching in various ester modes), 1614, 1500 cm^{-1} (–Ar). The ^{1}H NMR spectra of **A1**–**A3** showed peaks at 1.443–1.812, 2.380–4.154, 4.321–6.561 and 6.951–8.158, corresponding to methyl, methylene, pyranose and aromatic rings, respectively.

The results of FT–IR, ^{1}H NMR spectroscopy and elementary analysis confirmed that the target compounds, **A1**–**A3** had been produced.

3.2 Optical rotation

Maltose is optically active in aqueous solution with a specific rotation of +136°. **A1**–**A3** also exhibited optical activity (in THF, c = 0.8 g L^{-1}), with a specific rotation of –22.50°, –25.56° and –34.53°, respectively. It is clear that the chiral core plays an important role to the optical activity of the SSCs. The absolute value of the specific rotation for **A1**–**A3** increased with terminal chain length in the side-arms. This may be attributed to the flexibility of the SSC.

3.3 Mesomorphic properties

According to results reported previously, **b1** is a non-LC side-arm, but **b2** and **b3** are nematic [33]. The thermal properties and phase behaviour of the SSCs **A1**–**A3** were investigated by DSC. The phase transition temperatures and corresponding enthalpy changes obtained over the first heating and cooling cycle are summarised in Table 1. The DSC curves are shown in Figure 1.

A1 was thus a non–LC SSC. It showed a melting transition at 169.4°C during the heating cycle and a crystal transition at 140.1°C during the cooling cycle. On the other hand, **A2** and **A3** were thermotropic enantiotropic SSLCs, respectively showing a melting transition at 148.7°C and 133.7°C, a clearing transition at 187.8°C and 186.5°C, and a mesomorphic region (ΔT_1) at around 39.0°C and 53.7°C, during the heating cycle. During the cooling cycle, the mesomorphic regions (ΔT_2) were 63.8°C and 107.0°C, respectively. This demonstrated that the SSC exhibited LC properties only when the side-arms had LC properties. Longer terminal chains gave the SSLC a lower melting temperature and wider mesomorphic regions. The mesomorphic regions in the cooling cycle were wider than those during heating. The reason for this may be that the SSLC is less prone to crystallise during the cooling cycle, due to the branching structure.

Grandjean and oily textures were observed in natural preparations of the mesomorphic phase for **A2** and **A3** during the heating and cooling cycle. When the isotropic state of **A3** was cooled to 195°C cholesteric droplets separated from the isotropic melt, as illustrated in Figure 2(a), in which the coexistence of Grandjean-like areas of the cholesteric phase can be seen. These domains coalesced, and eventually the oily texture completely filled the microscope field of view, as shown in Figure 2(b). When the sample was cooled further, a colourful Grandjean texture was observed, the different colours corresponding to twist states at different temperatures [35], as seen in Figure 2(c).

Table 1. Transition temperatures and mesophase type of star-shaped compounds **A1–A3**.

Sample	Transition temperature (°C) (corresponding enthalpy changes, J g^{-1}) Heating/cooling	ΔT_1 (°C)	ΔT_2 (°C)	Mesophase
A1	Cr 169.4 (77.74) I/I 140.1 (−79.5) Cr	—	—	—
A2	Cr 148.7 (13.68) ch 187.8 (1.95) I/I 181.8 (−2.25) ch 118.0 (−8.59) Cr	39.1	63.8	ch
A3	Cr 133.1 (18.11) ch 186.8 (2.31) I/I 195.3 (−3.02) ch 88.3 (−12.62) Cr	53.7	107.0	ch

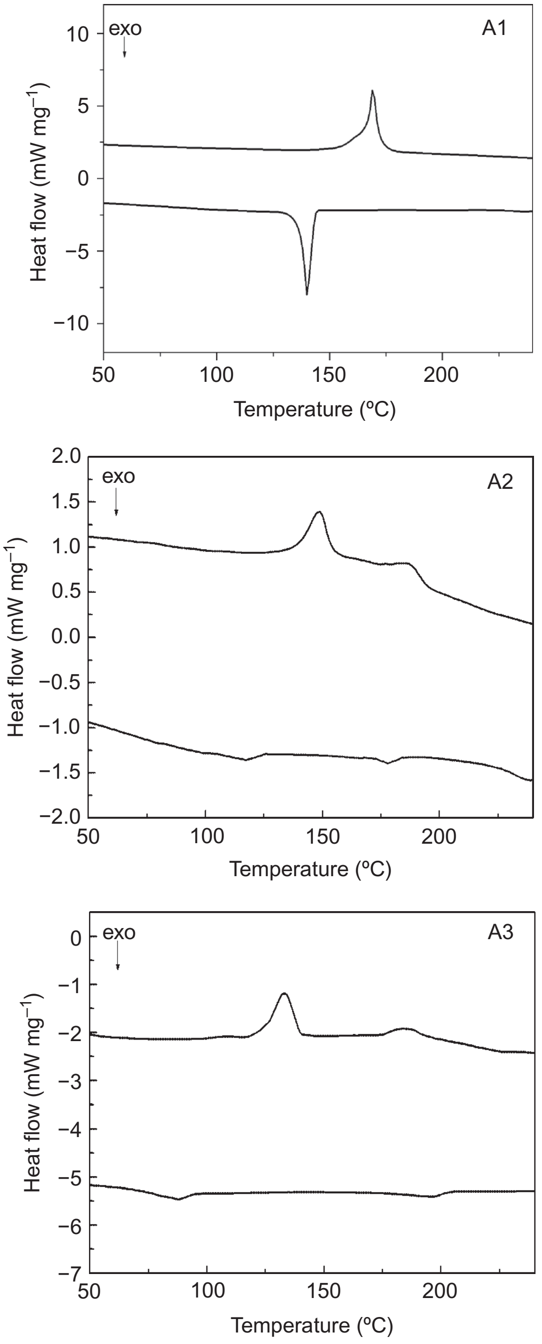

Figure 1. DSC thermograms of SSCs **A1**–**A3**.

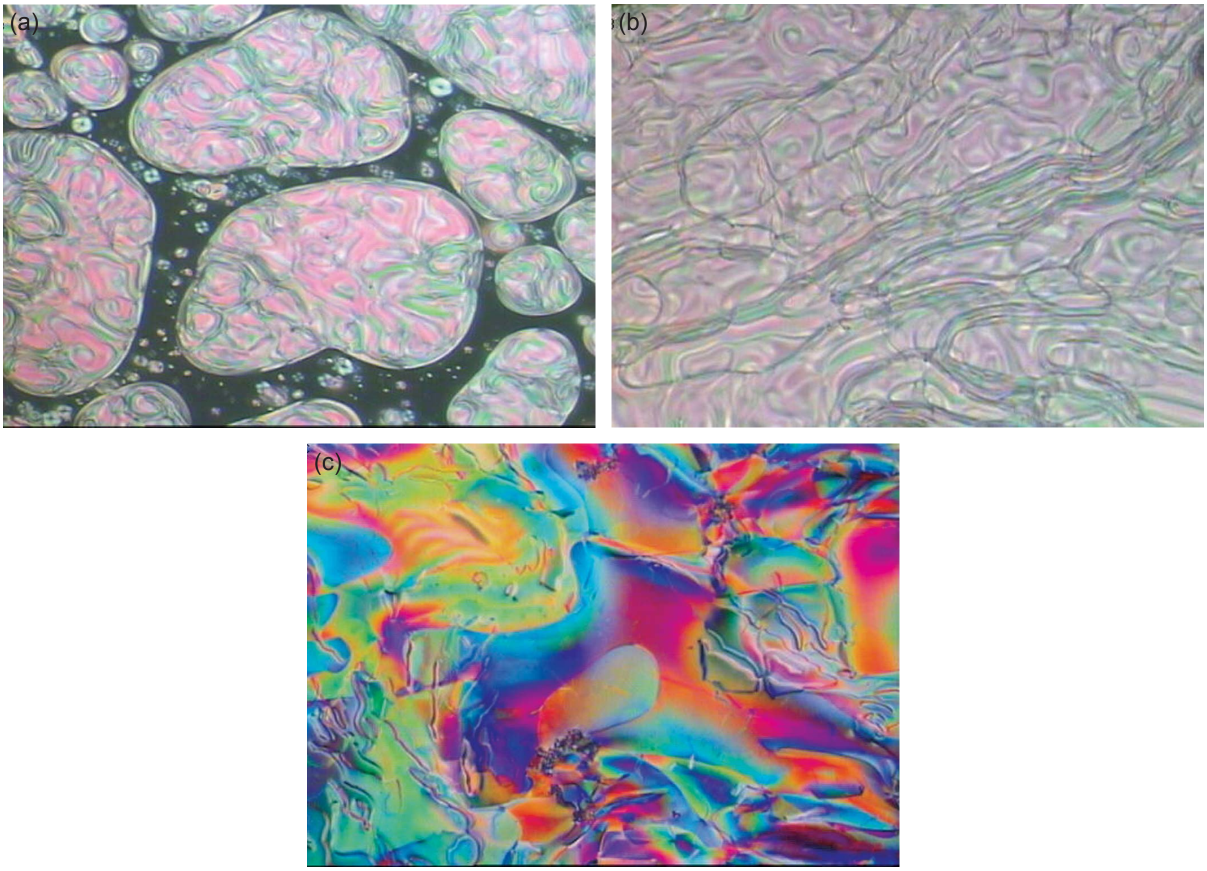

Figure 2. Polarising optical micrographs (200×) of **A3** during cooling: (a) at 195.0°C; (b) at 134.0°C; (c) at 107.0°C.

When the sample was cooled to 87°C the colourful texture slowly crystallised. Similar textures were observed in **A2**, in which Grandjean and oily texture were typical of the cholesteric phase. These results indicate that the cholesteric phase of an SSLC can be induced by maltose.

The unique optical properties of a cholesteric LC are related to the helical supramolecular structure of the cholesteric phase. The periodic helical structure of the cholesteric phase selectively reflects visible light in a similar manner to an ordinary diffraction grating, and the pitch controls the wavelength of the reflected light. If the reflected wavelength lies in the visible area of the spectrum, the cholesteric phase exhibits brilliant colours. Transmitted light shows the complementary colour. The wavelength of reflected light, λ_m, obeys the Bragg condition,

$$\lambda_m = nP, \tag{1}$$

where n is the average index of refraction and P is the pitch of the cholesteric phase, defined as the spatial distance over which the director rotates by 360°. The helical pitch is an important parameter in connection with optical properties of the cholesteric phase. Although the microscopic origins of the helical pitch are still a subject of study, it is known that the helical pitch and optical properties of cholesteric LC polymers depend mainly on the polymer backbone, the rigidity of mesogenic units, the length of the flexible spacer, and external conditions such as concentration, temperature, force field, electric field and magnetic field. In the present study maltose derivatives did not exhibit selective reflection in the visible light region.

XRD studies were carried out to obtain more detailed information on the LC phase structures and types. In general, a sharp and strong peak at low angle ($1° < 2\theta < 4°$) in the small angle X-ray scattering (SAXS) curve and a broad peak associated with lateral packing at $2\theta \approx 20°$ in the wide angle X-ray diffraction (WAXD) curve could be observed for the smectic structure. In the case of the nematic structure, no peak appeared in the SAXS curve, but in the WAXD curve a broad peak at $2\theta \approx 20°$ was observed. Similarly, in the case of the cholesteric structure no peak appeared

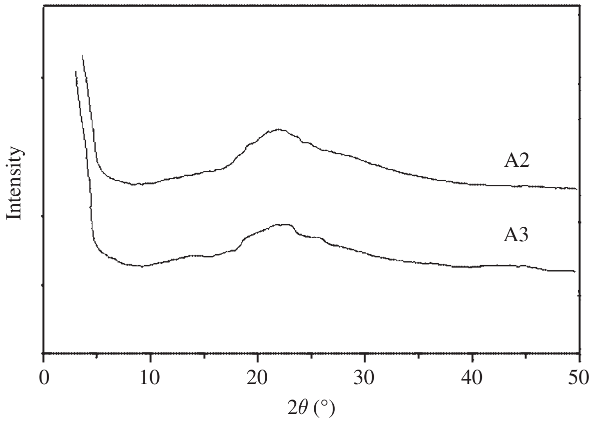

Figure 3. X–ray diffraction patterns of **A2** and **A3**.

in the SAXS curve. However, a broad peak was seen at $2\theta \approx 16$–18° or 20°.

The quenched samples of **A2** and **A3** were also studied by SAXS and WAXS. A diffuse peak around $2\theta = 22.5°$ was observed in the WAXD curves for **A2** and **A3**, and there was no sharp peak at low angles (Figure 3). The XDR data were consistent with their optical textures, and confirmed that **A2** and **A3** were indeed cholesteric SSLCs.

4. Conclusions

Three esters of maltose with 4-(4-(alkoxybenzoyloxy) phenoxy)-6-oxohexanoic acid side-arms have been synthesised. The influence on SSC properties played by the maltose core and the nature of the side-arms has been studied. The side-arm, **b1,** was non-LC in nature, but **b2** and **b3** were thermotropic nematic LCs. The SSC **A1** was non-liquid crystalline, but **A2** and **A3** were thermotropic LCs. These results demonstrated that the SSC displayed LC properties only when the side-arms were LC. Apart from their side-arms, the SSLCs **A2** and **A3** were cholesteric, and displayed Grandjean and oily textures in the cholesteric phase. The results indicate that the maltose core induced the cholesteric phase in the SSLCs with nematic side-arms. The mesomorphic region of the SSLC increased with terminal chain length, and these regions were wider during the cooling than the heating cycle.

Acknowledgements

The authors are grateful to the National Natural Science Fundamental Committee of China and the Fundamental Research Funds for the Central Universities (N100405005), and also to the Science and Technology Department of Liaoning Province for financial support of this work.

References

[1] Peter, P.M. *Nature* **1998**, *391*, 745.
[2] Chong, T.T.; Heidelberg, T.; Hashim, R.; Gary, S. *Liq. Cryst*. **2007**, *34*, 267–287.
[3] Vill, V.; Bocker, T.; Thiem, J.; Fischer, F. *Liq. Cryst*. **2006**, *33*, 1353–1358.
[4] Brettar, J.; Bürgi, T.; Donnio, B.; Guillon, D.; Klappert, R.; Scharf, T.; Deschenaux, R. *Adv. Funct. Mater*. **2006**, *16*, 260–267.
[5] Yao, D.S.; Zhang, B.Y.; Zhang, W.W.; Tian. M. *J. Mol. Struct*. **2008**, *881*, 83–89.
[6] Judele, R.; Laschat, S.; Baro, A.; Nimtz, M. *Tetrahedron* **2006**, *62*, 9681–9687.
[7] Zhang, B.Y.; Yao, D.S.; Meng, F.B.; Li, Y.H. *J. Mol. Struct*. **2005**, *741*, 135–140.
[8] Meier, H.; Lehmann, M.; Holst, H.C. *Tetrahedron* **2004**, *60*, 6881–6888.
[9] Liu, H.J.; Zhang, Q.Z.; Zhang, J.Z. *Mater. Lett*. **2005**, *59*, 2531–2534.
[10] Saezz, I.M.; Goodby, J.W. *Chem. Eur. J*. **2003**, *9*, 4869–4877.
[11] Lehmann, M.; Jahr, M.; Donnio, B.; Graf, R.; Gemming, S.; Popov, I. *Chem. Eur. J*. **2008**, *14*, 3562–3576.
[12] Suresh, K.I.; Tamboli, J.R.; Rao, B.S.; Verma, S.; Unnikrishnan, G. *Polym. Adv. Technol*. **2008**, *19*, 1323–1333.
[13] Pugh, C.; Kasko, A.M.; Grunwald, S.R. *J. Polym. Sci., Part A: Polym. Chem*. **2008**, *46*, 4363–4382.
[14] Kim, B.G.; Kim, S.; Park, S.Y. *Tetrahedron Lett*. **2001**, *42*, 2697–2699.
[15] Kuo, C.J.; Cheng, S.J.; Chang, S.T. *J. Org. Chem*. **2008**, *73*, 485–490.
[16] Abd-El-Aziz, A.S.; Carruthers, S.A.; Aguiar, P.M.; Kroeker, S. *J. Inorg. Organomet. Polym. Mater*. **2005**, *15*, 349–359.
[17] Lehmann, M.; Gearba, R.I.; Koch, M.H.J.; Ivanov, D.A. *Chem. Mater*. **2004**, *16*, 374–376.
[18] Lehmann, M.; Jahr, M.; Grozema, F.C.; Abellon, R.D.; Siebbeles, L.D.A.; Muller, M. *Adv. Mater*. **2008**, *20*, 4414–4418.
[19] Mormann, W.; Kuckertz, C. *Macromol. Symp*. **2002**, *181*, 113–122.
[20] Shi, M.; Zhang, H.L.; Chen, J.; Wan, X.; Zhou, Q. *Polym. Bull*. **2004**, *52*, 401–408.
[21] Bubnov, A.; Hamplov, V.; Kaspar, M.; Vajda, A.; Stojanovic, M.; Obadovic, D.Z.; Eber, N.; Fodor-Csorba, K. *J. Therm. Anal. Calorim*. **2007**, *90*, 431–441.
[22] Wang, X.Z.; Zhang, H.L.; Shi, D.C.; Chen, J.F.; Wang, X.Y.; Zhou, Q.F. *Eur. Polym. J*. **2005**, *41*, 933–940.
[23] Zelcer, A.; Donnio, B.; Bourgogne, C.; Cukiernik, F.D.; Guillon, D. *Chem. Mater*. **2007**, *19*, 1992–2006.
[24] Bisoyi, H.K.; Kumar, S. *Tetrahedron Lett*. **2008**, *49*, 3628–3631.
[25] Xu, J.W.; Ling, T.C.; He, C.B. *J. Polym. Sci., Part A: Polym. Chem*. **2008**, *46*, 4691–4703.
[26] Galliot, C.; Prevote, D.; Caminade, A.M.; Majoral, J.P. *J. Am. Chem. Soc*. **1995**, *117*, 5470–5476.

[27] Majoral, J.P.; Caminade, A.M. *Chem. Rev*. **1999**, *99*, 845–880.

[28] Galliot, C.; Larre, C.; Caminade, A.M.; Majoral, J.P. *Science* **1997**, *277*, 1981–1984.

[29] Yao, D.S.; Zhang, B.Y.; Li, Y.H. *Tetrahedron Lett*. **2004**, *45*, 8953–8956.

[30] Cheng, X.H.; Diele, S.; Tschierske, C. *Angew. Chem., Int. Ed*. **2000**, *39*, 592–595.

[31] Zhang, B.Y.; Xiao, W.Q.; Cong, Y.H. *Liq. Cryst*. **2007**, *34*, 1129–1136.

[32] Green, M.M.; Cheon, K.S.; Yang, S.Y.; Park, J.W.; Swansburg, S.; Liu, W.H. *Acc. Chem. Res*. **2001**, *34*, 672–680.

[33] Tian, M.; Zhang, B.Y.; Cong, Y.H.; Zhang, B. *J. Mol. Struct*. **2009**, *937*, 131–135.

[34] Tian, M.; Zhang, B.Y.; Cong, Y.H.; Zhang, N.; Yao, D.S. *J. Mol. Struct*. **2009**, *923*, 39–44.

[35] Dierking, I. *Textures of Liquid Crystals*; Wiley-VCH Verlag: Weinheim, 2003; p 80.